Predicting human inhibitory control from brain structural MRI

Ningning He[1]; Edmund T. Rolls[2,3]; Wei Zhao[1]; Shuixia Guo[1*]

1. MOE-LCSM, School of Mathematics and Statistics, Hunan Normal University, Changsha, P. R. China.

2. Oxford Centre for Computational Neuroscience, Oxford, England.

3. University of Warwick, Department of Computer Science, Coventry, England.

***Corresponding author:** Professor Shuixia Guo, School of Mathematics and Statistics, Hunan Normal University, Changsha 410006, China.

Tel.: +8613107019688
E-mail: guoshuixia75@163.com (Shuixia Guo)

Word count abstract: 287

Figures: 4

Supplemental material: 1.

[1] Abbreviations

[1] CPM, connectome-based predictive model; L.MTG, left middle temporal gyrus; MAPE, mean absolute percentage error; R.OFCmed, right medial orbitofrontal; sMRI, structural magnetic resonance imaging

Abstract

The anatomical structure of the human brain varies widely, as does individual cognitive behavior. It is important and interesting to study the relationship between brain structure and cognitive behavior. There has however been little previous work on the relationship between inhibitory control and brain structure. The goal of this study was to elucidate possible cortical markers related to inhibitory control using structural magnetic resonance imaging (sMRI) data. In this study, we analyzed sMRI data and inhibitory control behavior measurement values from 361 healthy adults from Human Connectome Project (HCP). Data of all subjects were divided into two datasets. In the first dataset, we first constructed individual brain morphometric similarity networks by calculating the inter-regional statistical similarity relationship of nine cortical characteristic measures (such as volume) for each brain area obtained from sMRI data. Areas that covary in their morphology are termed 'connected'. After that, we used a brain connectome-based predictive model (CPM) to search for 'connected' brain areas that were significantly related to inhibitory control. This is a purely data-driven method with built-in cross-validation. Two different 'connected' patterns were observed for high and low inhibitory control networks. The high inhibitory control network comprised 25 'connections' (edges between nodes), mostly involving nodes in the prefrontal and especially orbitofrontal cortex and inferior frontal gyrus. In the low inhibitory control network, nodes were scattered between parietal, occipital and limbic areas. Furthermore, these ‘connections’ were verified as reliable and generalizable on the second dataset. Two regions of interest, the right ventromedial prefrontal cortex including a part of medial area 10 (R.OFCmed) and left middle temporal gyrus (L.MTG) were crucial nodes in the two networks, respectively, which suggests that these two regions may be fundamentally involved in inhibitory control. Our findings potentially help to understand the relationship between areas with a correlated cortical structure and inhibitory control, and further help to reveal the brain systems related to inhibition and its disorders.

Keywords: Inhibitory control; Right medial orbitofrontal cortex; Left middle temporal gyrus; Morphometric similarity networks

1. Introduction

Inhibitory control (or response inhibition) is an executive function that permits an individual to inhibit their impulses and natural, habitual, or dominant behavioral responses to stimuli in order to select a more appropriate behavior that is consistent with completing their goals,including goals from the cognition domain (Diamond, 2013; Ilieva et al., 2015). An example of Inhibitory control is self-control, successfully suppressing the natural behavioral response to eat cake when one is craving it (Diamond, 2013). Many researchers believe that impaired inhibitory control is associated with brain disorders such as addiction and attention deficit hyperactivity disorder (Colzato et al., 2011; Fillmore & Rush, 2002; Dong et al., 2012; Koob & Volkow, 2010; Mostofsky et al., 2003; Liddle et al., 2010). The discussion of human Inhibitory control mechanisms has been one of the most intriguing issues in contemporary developmental cognitive neuroscience (Morasch et al., 2011; Watson & Bell, 2013; Pires et al., 2014; Maij et al.,2017).

One of the goals of modern neuroscience is to study the relationship between brain structure and function and the behavior of the individual. Technological advances in the field of brain research have accelerated the study of the relationship between the human brain and behavior. For example, sMRI can provide useful information about the anatomical structure of the brain and its differences in different individuals (Giedd, 2004). Structural brain imaging can be used to search for reliable and stable structural biomarkers, and also to explore the changes of brain structure that may be produced by cognitive training such as learning (Durston et al.,2001; Sowell et al., 2007). There have been many studies using structural imaging data to explore the relationship between brain structure and cognitive function. For example, a structural imaging data study showed significant differences in gray matter volumes in some areas of the brain in developing children with different cognitive functions (Yokota et al. 2015). Another study showed that changes in gray matter volume in individual brain regions are related to their social cognitive abilities (Hoekzema et al., 2016). Geisler et al showed a significant correlation between several types of cognitive decline in patients with schizophrenia and specific patterns of structural changes in certain brain regions (Geisler et al., 2015). In addition, many studies provide evidence that many brain regions in people with cognitive impairment, such as Alzheimer's disease, have varying degrees of atrophy compared to normal controls (Lim et al., 2012; Shimoda et al., 2015; Qi et al., 2017).

There has however been little previous work on structural correlates of inhibitory control, which is the aim of the present study. Measures of cerebral structure include regional volume, surface area, and curvature. Changes in these measures are usually related to each other, especially for surface area, the volume of gray matter, and mean cortical thickness (Rimol et al., 2012; Abé et al., 2016). Beyond this, Seidlitz et al

proposed a novel method for realizing the construction of an individual-based morphometric similarity matrix through a combination of morphometric features. Inter-regional 'connections' (in fact, similarity of structure) are estimated using newly introduced feature vectors, namely, the Pearson correlation coefficient of the concatenation of morphometric features, instead of one or two anatomical features (Seidlitz et al., 2018). Brain regions in which the feature vectors correlate when measured across a large set of individuals are said to have 'high connectivity', though in fact this represents covariation of structure (Li et al, 2017). There is emerging evidence that the combined analysis of multiple indexes is more effective than that of a single index (Glasser et al., 2011; Sabuncu et al., 2016; Vandekar et al., 2016; Whitaker et al., 2017; Seidlitz et al., 2018). Further, this method of constructing individual-based morphometric similarity networks has successfully improved the accuracy of discriminant analysis (Yu et al., 2018). Based on the above evidence, we predicted that the relationship between human inhibitory control and brain structure could be well studied by the new network construction method.

In this paper, we aimed to study whether individual inhibitory control is related to individual brain structure patterns. Inhibitory control ability was measured using scores on the flanker inhibitory control and attention test, as used in the HCP. The neuroanatomical features were measured by individual-based morphometric similarity networks constructed from nine cortical characteristic indexes between the brain regions as described by Li et al. (2017). We used a brain CPM to search for brain 'connections' significantly related to individual inhibitory control ability, which is a purely data-driven linear predictive model. It is important to note that this method uses cross-validation, which makes the inference of results more conservative and rigorous, thereby rendering our results more reliable. The results show that individual inhibitory control ability can be predicted by the morphometric similarity of brain regions in the prefrontal cortex, especially the orbitofrontal cortex and the inferior frontal gyrus. People with high inhibitory control were marked by a higher similarity measure for prefrontal cortical regions, especially the right medial orbitofrontal cortex (as defined in the Desikan-Killiany atlas (Desikan et al., 2006). These findings potentially help to understand the neuroanatomical basis of human inhibitory control, and further help to reveal the relationship between individual brain structure and inhibitory control ability.

2. Materials and methods

2.1 Participants and data acquisition

Data from HCP were collected from 361 adult subjects (177 males and 184 females), released by the WU-Minn HCP consortium. Here, we divided all of subjects' data into two datasets. The first dataset consisting of 214 subjects (112 males and 102 females, age mean±std: 28.7±3.8) was used to perform the main prediction analysis, while the second

dataset consisting of 147 subjects (65 males and 82 females, age mean±std: 29.2±3.6)) was used for validation analysis. All subjects were healthy and had no history of mental or neurological diseases. The inclusion information is given in Van Essen et al. (2013). All HCP subjects were scanned on a customized Siemens 3T housed at Washington University, using a magnetization-prepared rapid gradient echo (MPRAGE) sequence to acquire high-resolution sMRI, with repetition time = 2400ms, echo time = 2.14ms, inversion time = 1000ms, flip angle = 8°, resolution matrix = 224 × 224, voxel size = 0.7 × 0.7 × 0.7mm^3. The HCP Consortium obtained informed consent from all participants, and research procedures and ethical guidelines were followed in accordance with the Institutional Review Boards.

We used inhibitory control behaviour scores, which measure participants' attention and inhibitory control (Smid et al., 1996; Weintraub et al., 2013; Gershon et al., 2013). The flanker inhibitory control and attention test was designed and carried out by staff in the HCP and the test scores came from the HCP's release behavior data (https://db.humanconnectome.org/). Details on these scores and their interpretation are available in the NIH Toolbox Scoring and Interpretation Guide (Weintraub et al., 2013; Lerman et al., 2017). In brief, the flanker test was as follows. All of the instructions were displayed on a computer screen. The participants were told that there were five arrows and two buttons on the screen. These five arrows were in a row and pointed in the same or different directions. The participants were required to select the button with the same direction as the middle arrow (that is, the third arrow). Four practice trials were conducted during the preparatory phase. During the test phase, each participant took approximately 3 minutes to accomplish 20 trials. The total test score was equal to the sum of accuracy score and reaction time score (http://www.healthmeasures.net/explore-measurement-systems/nih-toolbox), where the accuracy score was equal to the number of correct responses divided by eight, and the reaction time score was computed with the following formula (Weintraub et al., 2013),

$$\text{reaction time score} = 5 - \left(5 * \left(\frac{\log t - \log 500}{\log 3000 - \log 500} \right) \right),$$

where t represents the reaction time for any experiment, minimum reaction time was 500 ms and maximum reaction time was 3,000 ms. This measure has become established in a number of other investigations (Zelazo et al., 2013; Zelazo et al., 2014; Heaton et al., 2014; Lerman et al., 2017; Wong et al., 2019). The inhibitory control ability score ranged from 71 to 121, and the median value was 99.04. Detailed information on the measured values of the participants is provided in Figure S1.

2.2 Data pre-processing

All subjects' sMRI data were pre-processed using FreeSurfer 5.3.0 (http://surfer.nmr.mgh.harvard.edu/), which is a magnetic resonance data processing software developed by MIT Health Sciences &Technology and Massachusetts General Hospital in the United States (Fischl, 2012). It provides a full processing stream for structural MRI data. First, skull stripping, B1 bias field correction, and gray-white matter segmentation were performed; then, cortical gray-white boundary surface and pial surface models were constructed. Next, regions on the cortical surface and subcortical brain structures were labeled. Finally, nonlinear registration of the cortical surface of an individual was performed with a stereotaxic atlas and the regional measurements (described in Dale et al., 1999). A total of nine brain morphological indexes were extracted, and each index depicted different cortical characteristics (Li et al., 2017). These were the number of vertices, the surface area, the volume of gray matter, the average and standard deviation of cortical thickness, the mean curvature, the Gaussian curvature, the curvature index, and the folding index. The number of vertices and the surface area were measured using the surface model. In the surface model, the cortical surface was divided into a small adjacent triangle; the number of vertices and the surface area were calculated by calculating the number of vertices and the area of triangles, respectively (Panizzon et al., 2009). The volume of gray matter was measured using the volume model. In the volume model, the cortex is divided into a cube, each representing an individual element, and the volume of gray matter is calculated by calculating the number of voxels within the region. The mean cortical thickness was the average of the distance between the cortical inner surface and the white matter surface at all vertices. The folding index was calculated by calculating the ratio of the sulcus-occluded cortex to the apparent cortex (Schaer et al., 2008, Schaer et al., 2012). The measurement of curvature represented the degree of curvature at a point in different directions (Pienaar et al., 2008; Li et al., 2014).

2.3 Brain morphometric similarity network construction

In this study, we used the Desikan-Killiany atlas (Desikan et al., 2006), which is based on the gyri and sulci and divides the brain into 68 brain regions (34 brain regions per hemisphere). For each subject's brain imaging, we first obtained data from 68 brain regions applying the above template. After data pre-processing, we next obtained nine morphological indexes for each brain region. To construct the brain network, we also defined the brain region as the nodes and the Pearson correlation coefficient between these morphological indexes of two brain regions as edges. Specifically, let $V_i = [A_{i1}, A_{i2}, \ldots, A_{i9}]$ be a brain region with nine cortical indexes $A_{i1}, A_{i2}, \ldots, A_{i9}$, $i = 1,2,\ldots,68$. What is worth mentioning is that each index was standardized to eliminate dimensions. Then, the bivariate correlation

coefficients $\rho(V_i,V_j)$ were calculated between each pair of brain regions,

$$\rho(V_i,V_j)=\frac{\mathrm{cov}(V_i,V_j)}{\sqrt{Var(V_i)}\sqrt{Var(V_j)}},$$

where $\mathrm{cov}(V_i,V_j)$ denote the covariance between the indexes of brain region V_i and V_j , $j=1,2,\ldots,68$; it reflects the variability among the indexes; $Var(V_i)$ denote the variance of the indexes of brain region V_i . Finally, an individual brain morphometric similarity network consisting of 68 brain regions (nodes) and 2278 edges ('connections') was obtained. We repeated the above steps and finally obtained each subject's individual brain morphometric similarity network.

2.4 Predicting inhibitory control ability by the brain connectome

In this study, we used the brain CPM, which is a data-driven approach to establish a brain-behavioral relationship prediction model from brain connection data using cross-validation (Shen et al., 2017). In the first dataset, the goal was to establish a linear relationship between brain connectivity data and behavioral measurements, which included five steps: 1) Data set partition: we used the leave-one-out cross-validation method. (To illustrate the stability of the method, we also used 10-fold cross-validation. Detailed descriptions are included in the supplemental material). For each iteration, one participant was cyclically retained as the test set, and the others were used as the training set. 2) Feature selection, which involved searching for all 2278 connections and selecting those connections associated with the behavioral measurements. To be specific, we first calculated the correlation coefficient between each connection and the behavioral score across the subjects in the training set. We selected those connections whose p-value was smaller than a given threshold. There has been no uniform standard for the selection of this threshold (Rosenberg et al., 2018; Shen et al., 2017; Beaty et al., 2018), so we decided to select a threshold range 0.01 to 0.05 with a step of 0.01, which was used to identify those connections significantly associated with the behavioral score. 3) Feature summation, which involved generalizing the magnitude of those connections significantly associated with the behavioral score and ensuring that the next step was modeled. For each morphometric similarity network in the training set, we summed the magnitude of those connections with significantly positive correlation and negative correlation, respectively. We used $xpos_i$ and $xneg_i$ to represent the summation of the significantly positive and negative correlation connection set of the i'th morphometric similarity network. 4) Model building, which assumed that there was a linear relationship between the

generalized value of the brain connection (independent variable, that is, $xpos_i$ and $xneg_i$) and the behavioral variable (dependent variable, we denoted it as y_i that is the i'th subject's behavioral score in the training set). The linear regression model was as follows, which included the age and gender of each subject as covariates.

$$Y = B_0 + B_1 * Xpos + B_2 * Xneg + B_3 * age + B_4 * gender + \varepsilon \qquad \text{(A)},$$

where $Y = [y_1, y_2, \ldots, y_n]^T$, $Xpos = [xpos_1, xpos_2, \ldots, xpos_n]^T$, $xpos_i$ represented the sum of the magnitude of the positively correlated connections of the i'th subject; $Xneg = [xneg_1, xneg_2, \ldots, xneg_n]^T$, $xneg_i$ represented the sum of the magnitude of the negatively correlated connections of the i'th subject; n was the number of the subject in the training set. B_i , $i = 0, \ldots, 4$ were the regression coefficients to be estimated. ε was the noise term. The regression coefficients of this multiple linear regression were estimated by a least squares method. We obtained the evaluation values $\hat{B}_i, i = 0, \ldots, 4$.

5) Model assessment, which involved comparing the prediction values with the observed values. In the previous step, we obtained the linear prediction model,

$$\hat{Y} = \hat{B}_0 + \hat{B}_1 * Xpos + \hat{B}_2 * Xneg + \hat{B}_3 * age + \hat{B}_4 * gender \qquad \text{(B)}.$$

We then applied this model to the test set. Firstly, we found those significantly positive and negative correlation connections in the morphometric similarity network of subjects in the test set and summed them, respectively. Then, we substituted them into the above regression equation to get the predicted behavioral scores $\hat{Y}$. To assess the prediction results, we calculated the correlation coefficient between the predicted behavioral scores and the observed behavioral scores $\rho(Y, \hat{Y})$, and performed a hypothesis test of the correlation coefficient. Concurrently, the mean absolute percentage error (MAPE) of the prediction model was calculated (Tofallis, 2015), which was equal to the average of the absolute value of the residuals of real observation values and the predicted values of the model, and the formula is as follows,

$$MAPE = \frac{1}{\mathrm{n}} \sum_{i=1}^{n} \frac{|y_i - \hat{y}_i|}{y_i} ,$$

where n was the number of the model (that is, the number of all subjects because of the

leave-one-out cross-validation); y_i was the observed behavioral score; and $\hat{y}_i$ was the predicted behavioral score. Using each of the feature selection thresholds, we obtained a regression model and its predictive evaluation indicators, which were the correlation coefficient $\rho(Y,\hat{Y})$ and MAPE of the model. Corresponding to five thresholds, we obtained a total of five prediction models. The optimal model was selected according to the predictive evaluation indicators. A flowchart of the process of constructing the prediction model from the raw data is shown in Figure S2.

Considering that there were two kinds of relationship between brain connections and inhibitory control ability, positive correlations and negative correlations, we also performed the above model construction and evaluation process by taking the summation of the positive or negative correlation connection set as an independent variable, respectively, under the optional feature selection threshold.

In addition, due to cross validation, it was possible to select a slightly different connection set in each iteration under the optimal feature selection threshold, but the connections most related to the behaviour measurement value should appear in different iterations, so we identified these connections selected in all iterations which formed a shared connection set. Similarly, the summarized values of the shared positive connections and shared negative connections were calculated and then used as independent variables to fit the linear prediction model,

$$Y = B_0 + B_1 * SXpos + B_2 * SXneg + B_3 * age + B_4 * gender + \varepsilon \qquad \text{(C)},$$

where $Y = [y_1, y_2, \cdots, y_n]^T$, $SXpos = [sxpos_1, sxpos_2, \cdots, sxpos_n]^T$, $sxpos_i$ represented the sum of the magnitude of the shared positive connections of the i'th subject; $SXneg = [sxneg_1, sxneg_2, \cdots, sxneg_n]^T$, $sxneg_i$ represented the sum of the magnitude of the shared negative connections of the i'th subject; n was the number of the subject. B_i, $i = 0, \cdots, 4$ were the regression coefficients to be estimated. ε was the noise term. Subsequently, we used leave-one-out cross-validation to estimate the model parameters on the training set and predict the inhibitory control ability score on the test set. Finally, the prediction results were evaluated.

2.5 Validation analysis on independent dataset

We used the second independent dataset for verifying the reliability of the above model performing on the first dataset. Specifically, taking the first dataset as the training set, we fitted a brain connection prediction model using shared connections that identified in the

previous section, with age and gender as covariables. After that, with the second data set as the testing set, we used the prediction model to predict the inhibitory control ability scores of all 147 subjects. We calculated the correlation coefficient between the predicted behavioral scores and the observed behavioral scores to assess the prediction results.

2.6 Permutation test

After calculating the correlation coefficient between the observed behaviour score and the predicted behaviour score obtained by any model, a non-parametric permutation test was performed to test whether the relationship was significantly better than random. Specifically, we first randomly redistributed the behavior scores across all subjects, which broke the real brain connection-behaviour relationship. We then used CPM to establish a linear relationship between brain connectivity data and random behavioral measurements. The process was repeated 1000 times and then we obtained the empirical distribution of the correlation coefficients, which were used to test the significance of the correlation coefficients.

3. Results

3.1 Prediction of inhibitory control ability with positive and negative connection sets

Based on the purely data-driven method, we first calculated the correlation coefficient of each of the 2278 edges with the inhibitory control ability scores. Given the threshold, we next selected edges whose p values were smaller than the threshold value and then used the selected edges to construct the prediction model. Because there is no unified standard for the selection of the threshold value in the previous literature, we selected a threshold range from 0.01 to 0.05. The results showed that when the threshold value was 0.01, the correlation coefficient between the observed and predicted inhibitory control ability scores obtained by using prediction model B was 0.32 ($p = 1.31 \times 10^{-6}$, Figure 1). After a non-parametric permutation test, it was observed that the real brain connection-inhibitory control ability relationship was significantly better than that of the random ones (permutation test, $n = 1000$, $p < 0.001$). The MAPE of the prediction model was 8.5%, indicating that the accuracy of the model was 91.5%. When the threshold value was equal to 0.02, the correlation coefficient between the observed and predicted inhibitory control ability scores was 0.25 ($p = 2.9 \times 10^{-4}$), and the accuracy of the model was 91.1%. For the other threshold values, the prediction result of model B was slightly worse than the results when using 0.01 as the threshold. The detailed results are included in Figure S3.

Our results show that the optimal threshold was equal to 0.01, that is, the connections selected by the optimal threshold were those most related to inhibitory control ability. Figure S4 showed the prediction results of the models obtained by using the positive or negative connection set under the optimal threshold.

3.2 Results of the shared connections set

Under the optimal feature selection threshold, we defined those edges that were selected using model A in all iterations of cross validation as shared connections. The results revealed that a total of 48 edges were defined as shared connections; 25 shared connections were positively correlated and 23 shared connections were negatively correlated with inhibitory control ability scores. They comprise what we term the high and low inhibitory control networks, respectively, which are shown in Figure 2 https://bioimagesuiteweb.github.io/webapp/connviewer.htm. The network module in Figure 2 was defined by the Power atlas (Power et al. 2011), and by the Desikan-Killiany atlas (Desikan et al., 2006). In Table S2, we list all 68 brain regions and the networks to which each brain region belongs. In the high inhibitory control network, it was clear that R.OFCmed had the highest degree. Eight of the 25 connections were connected to R.OFCmed, which was mostly connected to the nodes in the prefrontal cortex. In the low inhibitory control network, we observed that L.MTG had the highest degree and R.OFCmed had the second highest degree. The nodes connected to R.OFCmed were scattered between parietal, occipital, and limbic modules. L.MTG was mostly connected to the nodes in the limbic module. The connection patterns were completely different between high and low inhibitory control networks. For clarity, we have drawn R.OFCmed and L.MTG on inflated surfaces (Figure 3). It is important to make it clear that OFCmed in the Desikan-Killiany atlas (Desikan et al., 2006) includes the gyrus rectus (area 14), the anterior cingulate cortex area 32 below the level of the genu of the corpus callosum but not 24, and cortex anterior to this including 10r, 10m and part of 10p according to the definition of Ongur, Ferry and Price (2003). These areas are sometimes described as the ventromedial prefrontal cortex. OFCmed in this atlas does not include any of the medial orbitofrontal cortex areas 11 and 13 (Rolls, 2019). Detailed information on shared connections is listed in Table S1.

3.3 Prediction of inhibitory control ability with shared connections

Using model C (of section 2.4) to explore the relationship between brain shared connections and inhibitory control ability, we found that the correlation coefficient between the observed and predicted scores was 0.54($p < 10^{-30}$, Figure 4). The results of the non-parametric permutation test showed that this relationship was significantly superior to random (permutation test, $n = 1000$, $p < 0.001$). In addition, the MAPE of the prediction model was 7.3%. Compared with the prediction results of model A, we found that using

shared connections as the predictor could improve the prediction accuracy.

3.4 Results of validation analysis

We explored the generalization of the prediction model by predicting on the second dataset. The correlation coefficient between the observed and predicted scores was 0.46($p = 6.36 \times 10^{-9}$). The results of the non-parametric permutation test showed that this relationship was significantly superior to random (permutation test, $n = 1000$, $p < 0.001$).

4. Discussion

In this study, we have shown that morphometric similarity of brain regions is a good predictor of individual inhibitory control ability. This new network construction method provided us with a new perspective to study the relationship between brain and individual cognitive behavior. Using a recently developed and data-driven prediction method, we found that the score of individual inhibitory control ability increased as the increasing similarity of prefrontal cortex. As theoretically predicted, individual differences in inhibitory control ability are related to individual differences in the morphometric similarity network.

4.1 Brain morphometric similarity network

In this work, nine indexes for characterizing cortical properties were extracted from the standard structural T1-weighted MRI data. Then, for each individual, the covariance between brain regional morphometric features was calculated for each possible pair of brain regions. After that we obtained the individual morphometric similarity network. Most of the morphometric similarity networks constructed in previous studies were based on single index and group level. However, different indexes depict different characteristics of the cortex. It is necessary to consider the cortical features in an all-round way. Li et al. (2017) proposed that the morphometric similarity network can be constructed by the above nine indexes and verified the feasibility of the method and the stability of the network. In this paper, we compared the predictive power of a single morphometric feature to the combination of 9 features**.** By using a single measure (such as the volume of each region) instead of the above morphological combination of features as the independent variable in the regression model, we found that the predictive power of a single morphometric feature not quite as good as the combination. The number of vertices, the surface area and the volume of gray matter have similar predictive power ($r = 0.26 \sim 0.27$), which is a little less than the predictive power of the combination of nine features ($r = 0.32$). The optimal prediction results for each measure are shown in Table S4. The results of this study showed that the combination of multiple indexes may be used as a new way to construct the individual morphometric similarity network. It also

implies that the basic organizational principle of the anatomical networks of the human brain is consistent with previous research on functional networks (He et al., 2007; Seidlitz et al., 2018).

4.2 High and low inhibitory control networks

On the basis of the method of brain CPM, we used connections that were selected for all iterations in cross validation under the optional feature selection threshold to build a prediction model. The results showed that the prediction model based on shared connections was better than the model based on positive and negative connections. Similar to the independent variable selection, we believe that shared connections are the best independent variables; i.e., the inhibitory control ability of the subjects could be best explained by high and low inhibitory control networks. We emphasize here that 'connections' refers here to correlations between the structure of different brain regions assessed across a group of participants.

We interpret some of the findings as follows. The measure used here of the similarity of a pair of cortical regions is whether the nine morphometric features are correlated with each other when measured across a large group of individuals. A high correlation of morphometric features might reflect a shared contribution of heredity in organising a group of brain areas that develop together in evolution perhaps as parts of a processing system, or might reflect common experience-related plasticity of a set of brain areas. In most cases in this investigation, a positive correlation with inhibitory control measured in the flanker task reflected a high positive correlation between the covariation of morphometric features of two brain areas, and inhibitory control ability, and vice versa. An implication from the network with positive correlations with inhibitory control ability (Figure 2) is that when parts of the orbitofrontal cortex and the cortex in the bank of the superior temporal sulcus (STS) covary and the middle temporal and middle frontal gyri, and some parietal areas and the posterior cingulate (PCC) covary in their morphology, then there is high inhibitory control ability. An implication from the network with negative correlations with inhibitory control ability (Figure 2) is that when parts of the orbitofrontal cortex have a negative covariation with the postcentral gurus (PoCG) and visual areas in their morphology, then there is high inhibitory control ability. That would imply that separation as a result of the effects of evolution or experience between these areas would facilitate inhibitory control.

Previous studies have emphasized the importance of the prefrontal region in inhibitory control, especially the inferior frontal gyrus and lateral orbitofrontal cortex (Metzuyanim et al., 2016; Rolls, 2017; Deng et al., 2017; Rolls, 2018). In our study, most of the brain areas involved in high inhibitory control network are located in prefrontal regions. In particular, we found that 13 of the 25 connections in this network involved prefrontal nodes. On the other hand, we found that the brain regions involved in the low inhibitory control network are scattered between parietal, occipital, and limbic modules.

The connection pattern of the low inhibitory control network is quite different from the high inhibitory control network. We can view these results as low inhibitory control ability may be marked by increased connections (covariation in morphology) between brain regions that do not support inhibitory control. According to previous studies based on functional imaging data, the prefrontal cortex is responsible for advanced cognitive function including working memory and attention (Luo et al., 2001; Rolls, 2016), and if a region within this module is damaged or cut off from other regions, cognition will be affected (Fuster, 2001). In a task-fMRI study, regions within the prefrontal cortex showed increased activation during inhibitory control tasks such as playing a violent game (Hummer et al., 2010). A meta-analysis of the various modules of functional connectivity networks found that the frontoparietal module focused on cognitive executive function (Crossley et al., 2013). The results provided evidence that high inhibitory control ability may be accompanied by highly developed prefrontal regions. In addition, prior functional connectivity MRI (fcMRI) studies have suggested that functional connectivity between the dorsolateral prefrontal cortex, inferior parietal lobule and dorsal anterior cingulate may have utility as a biomarker for individual differences in inhibitory control performance (Niendam et al., 2012; Stange et al., 2017). There is also growing evidence to support the hypothesis that changed functional connectivity within inhibitory control networks is associated with impaired inhibitory control in cannabis-dependent users (Filbey & Yezhuvath, 2013) and major depressive disorder (Stange et al., 2017). The above fcMRI studies investigated the inhibitory control network, which mainly revealed functional connectivity between brain regions in the prefrontal cortex and other regions. These results are consistent with the morphometric findings in our paper. Thus, better understanding of neural connections and neural networks in the brain will help to understand the mechanisms underlying diseases caused by their changes (Rolls, 2016).

4.3 The role of R.OFCmed and L.MTG in inhibitory control

The findings in this work highlight that inhibitory control can reliably be related to certain brain regions. We found that 22 of all 48 shared connections were related to R.OFCmed and L.MTG. The region of interest, R.OFCmed, had the highest degree of connectivity in shared connections, suggesting that it may be the target area that we were looking for that was closely related to inhibitory control. Previous evidence suggests that the lateral frontal cortex is responsible for high-level cognitive activity, which was more connected to other regions of the brain and determined the transmission of information and execution of cognitive functions (Neubert et al., 2014). A number of studies have found that damage to R.OFCmed leads to an inability to inhibitory control (Szatkowska et al., 2007; Walton et al., 2010; Izquierdo & Jentsch, 2012). An experimental study showed that the removal of gyrus rectus in the R.OFCmed cortex resulted in poor performance in tests that measured the inhibitory response and switching of stimulus and attention (Szatkowska et al., 2007). Another task-based study found that OFCmed cortex was necessary for evaluating and favouring future rewards to make a choice (Sellitto et al., 2010). Consistent with this,

impaired OFCmed cortex rendered patients more likely to be distracted by unrelated choices (Noonan et al., 2017). This ventromedial prefrontal cortex region is also implicated in decision-making between different rewards (Rolls, 2017, 2019). Therefore, we conclude that R.OFCmed cortex and its morphological connections to other brain regions provide an anatomical basis of inhibitory control ability. Another region of interest is L.MTG. It is worth noting that there was no overlap between the regions connected to L.MTG and the regions connected to R.OFCmed (Table S1). This suggests that they deal with different aspects of inhibitory control. The results of this paper emphasize the importance of these two brain regions to inhibitory control, which are shown from two perspectives in Figure 3. The results of this study provide evidence for the role of L.MTG in inhibitory control. Dong et al. (2012) found that internet addiction disorder demonstrated significantly greater 'Stroop' effect-related activity in the anterior and posterior cingulate cortices, as well as L.MTG compared with their healthy peers, which may suggest diminished efficiency of response-inhibition processes in the internet addiction disorder group. Another study suggested that activation reductions were seen in bilateral MTG of patients with transitioning to heavy use of alcohol at baseline during response inhibition (Norman et al., 2011). A functional MRI study suggested that activation reductions were seen in bilateral MTG of patients transitioning to heavy use of alcohol at baseline during the task of inhibitory control (Norman et al., 2011). Moreover, Hampshire & Sharp (2015) reviewed that response inhibition is a broader class of control processes that are supported by the same set of frontoparietal networks and these domain-general networks exert control by modulating local lateral inhibition processes, which occur ubiquitously throughout the cortex. It suggested that inhibitory control requires functional integration or separation of different brain regions rather than a single region and we postulate that the two regions (i.e., R.OFCmed and L.MTG) found in our paper might be key regions involved in the process of inhibitory control and this deserves further investigation.

5. Conclusions

Two important results were obtained in this study. The first was that all connections of the high inhibitory control network involved prefrontal cortex regions, which suggests that the prefrontal cortex may be related to inhibitory control ability. Secondly, we were interested in shared connections. We found that R.OFCmed had the highest degree of connections. These results emphasize the localization of inhibitory control function in brain networks and imply that R.OFCmed may be involved in inhibitory control. It may also be a target area closely related to inhibitory control, and dysfunction in this region may underlie the pathology of cognitive disorders in for example Alzheimer's disease.

6. Limitations

The study has some limitations. First, theoretically speaking, each calculation method of morphometric features has a certain degree of measurement error, and there may be

room for improvement in the algorithms used in the Freesurfer software. Second, we only considered a linear relationship between brain connections and behavioral values, but complex brain networks may require nonlinear explanations. Furthermore, in the process of feature combination, we adopted a simple summation calculation, which may affect the generalization value. Third, the use of the brain regions template by the Freesurfer software did not allow precise identification of which parts of the orbitofrontal cortex are related using this morphology measure to inhibitory control.

Conflicts of interest

All authors declare no competing interests.

Ethical approval

All procedures performed in studies involving human participants were in accordance with the ethical standards of the institutional or national research committee and with the 1964 Helsinki declaration and its later amendments or comparable ethical standards.

Acknowledgements

Use of the Human Connectome Project (https://www.humanconnectome.org/) dataset is acknowledged. Shuixia Guo is supported by the National Natural Science Foundation of China (NSFC) grant (No.11671129). All work of the study was done by the authors. The authors were responsible for the authenticity of the data and related results.

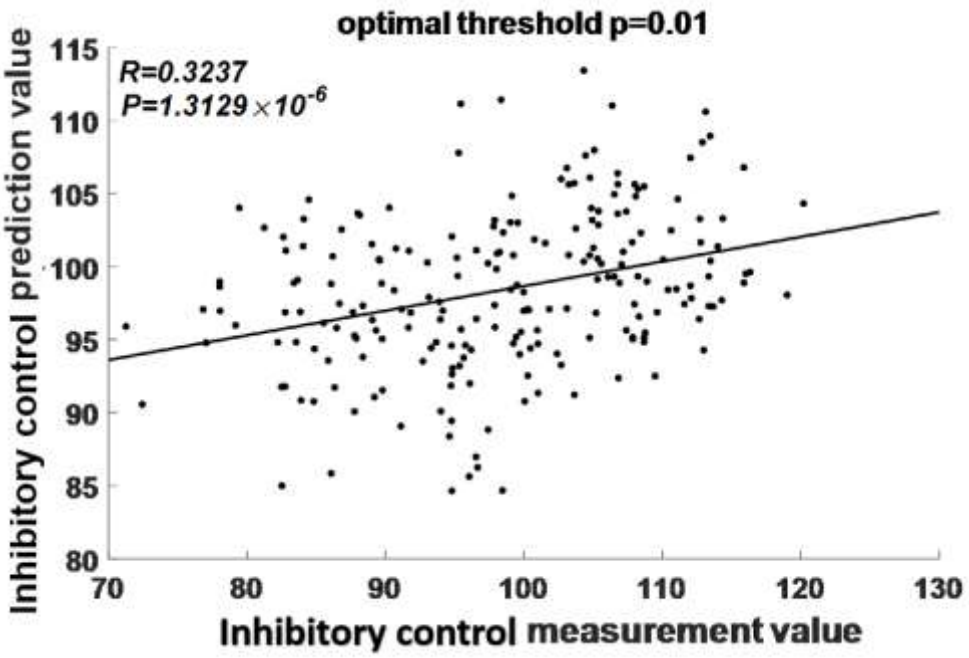

Figure 1. The result of predicting inhibitory control ability score with the positive and negative connection set under the optimal threshold. All subjects' observed and predicted inhibitory control ability scores are plotted in this figure. The correlation coefficient between the observed scores and the predicted scores was 0.32, which was significantly better than chance (permutation test, $n = 1000$, $p < 0.001$).

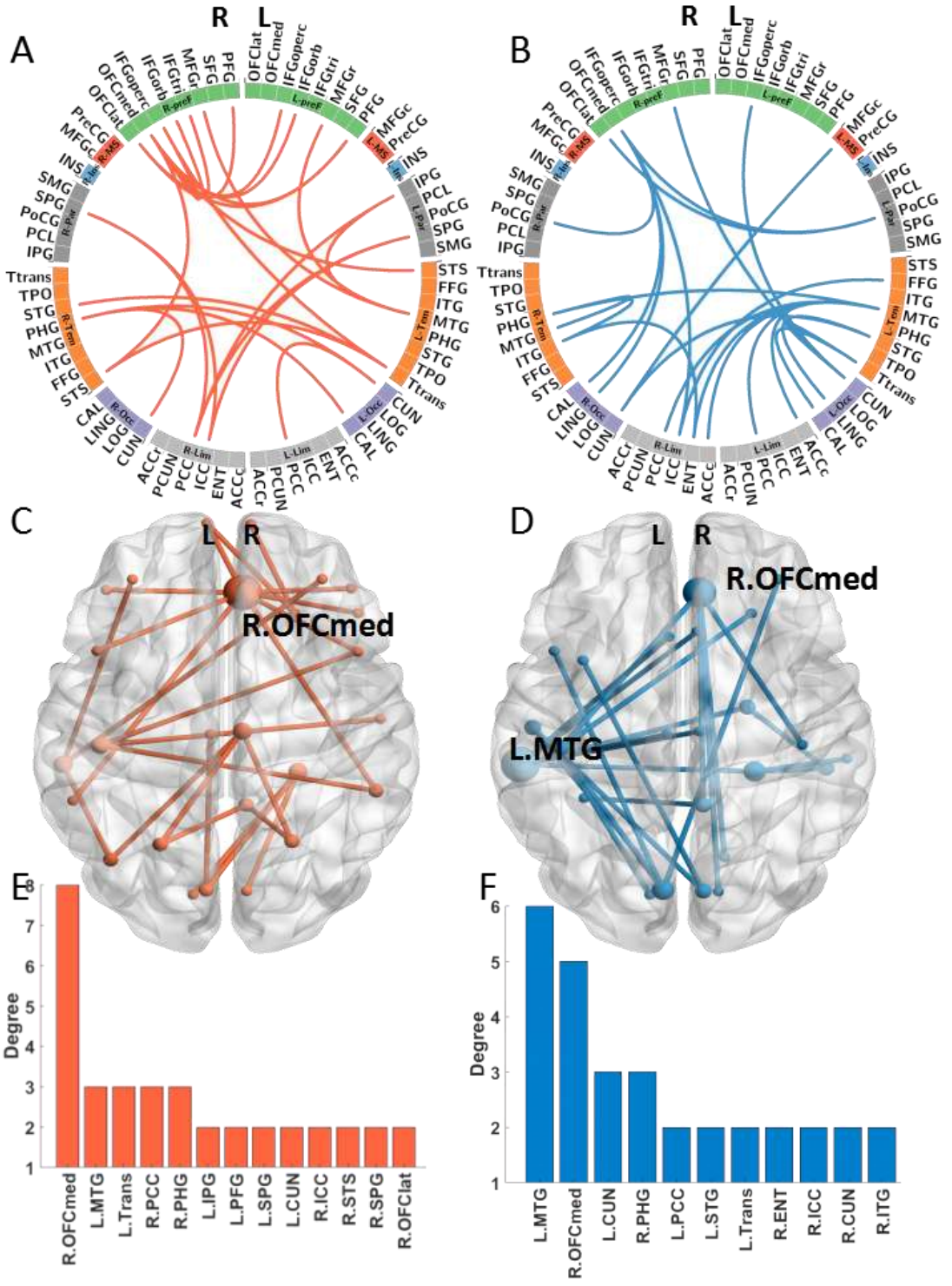

Figure 2. Visualization of shared connections. The positive shared connections are shown in red (A,C) (the negative shared connections in blue (B,D)). At the same time, these shared connections are shown in a 3D view (C,D). The two histograms show the degree of the brain regions in the high and low inhibitory control networks(E,F). See Table S4 for abbreviations.

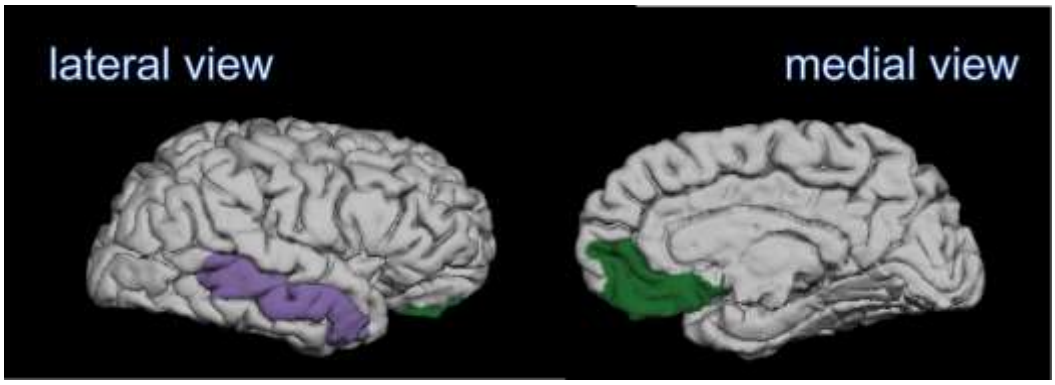

Figure 3. Visualization of the medial orbitofrontal cortex (OFCmed, green) and middle temporal gyrus (MTG, purple) on an inflated cortical surface.

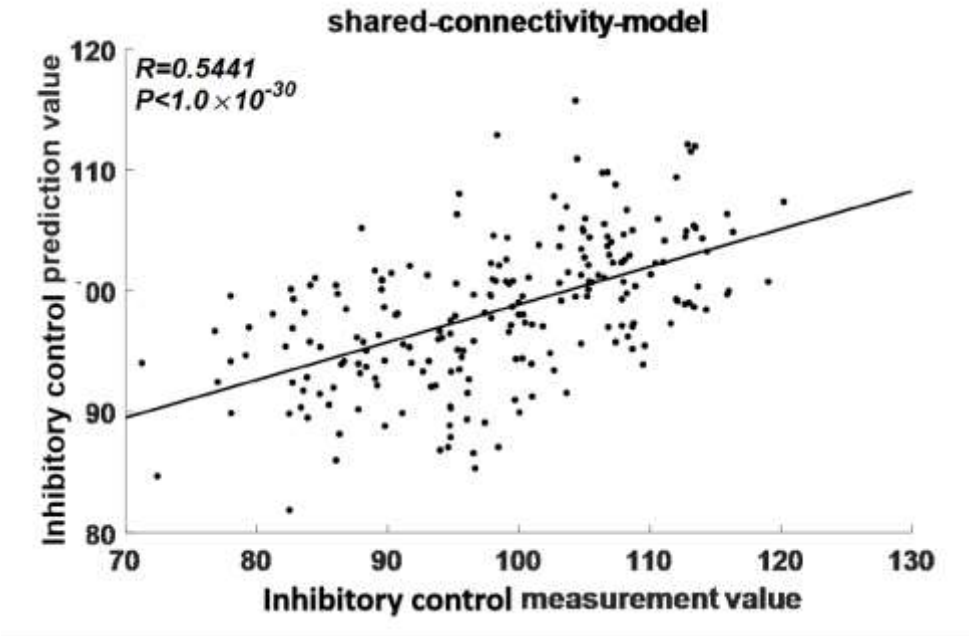

Figure 4. The result of predicting inhibitory control ability scores with shared connections. Shared connections are those connections selected in all iterations in cross-validation under the optional feature selection. All subjects' observed and predicted inhibitory control ability scores were plotted. The correlation coefficient between the observed scores and the predicted scores was 0.54, which was significantly better than random (permutation test, $n = 1000$, $p < 0.001$).

References

1. Abé, C., Ekman, C.-J., Sellgren, C., Petrovic, P., Ingvar, M., & Landén, M. (2016). Cortical thickness, volume and surface area in patients with bipolar disorder types I and II. Journal of Psychiatry & Neuroscience, 41(4), 240–250.

2. Beaty, R. E., Kenett, Y. N., Christensen, A. P., Rosenberg, M. D., Benedek, M., Chen, Q., … Silvia, P. J. (2018). Robust prediction of individual creative ability from brain functional connectivity. Proceedings of the National Academy of Sciences, 115(5), 1087–1092.

3. Colzato, L. S., Ruiz, M. J., van den Wildenberg, W. P. M., Bajo, M. T., & Hommel, B. (2011). Long-term effects of chronic khat use: Impaired inhibitory control. Frontiers in Psychology, 1.

4. Crossley, N. A., Mechelli, A., Vertes, P. E., Winton-Brown, T. T. Patel, A. X., Ginestet, C. E., … Bullmore, E. T. (2013). Cognitive relevance of the community structure of the human brain functional coactivation network. Proceedings of the National Academy of Sciences, 110(28), 11583–11588.

5. Dale, A. M., Fischl, B., & Sereno, M. I. (1999). Cortical surface-based analysis. NeuroImage, 9(2), 179–194.

6. Deng, W., Rolls, E. T., Ji, X., Robbins, T. W., Banaschewski, T., Bokde, A. L. W., … Feng, J. (2017). Separate neural systems for behavioral change and for emotional responses to failure during behavioral inhibition. Human Brain Mapping, 38: 3527–3537.

7. Desikan, R. S., Ségonne, F., Fischl, B., Quinn, B. T., Dickerson, B. C., Blacker, D., … Killiany, R. J. (2006). An automated labeling system for subdividing the human cerebral cortex on MRI scans into gyral based regions of interest. NeuroImage, 31(3), 968–980.

8. Diamond, A. (2013). Executive functions. Annual Review of Psychology, 64(1), 135–168.

9. Dong, G., DeVito, E. E., Du, X., & Cui, Z. (2012). Impaired inhibitory control in “internet addiction disorder”: A functional magnetic resonance imaging study. Psychiatry Research: Neuroimaging, 203(2-3), 153–158.

10. Durston, S., Hulshoff Pol, H. E., Casey, B. J., Giedd, J. N., Buitelaar, J. K., & Vanengeland, H. (2001). Anatomical MRI of the developing human brain: What have we learned? Journal of the American Academy of Child and Adolescent Psychiatry, 40(9), 1012–1020.

11. Filbey, F., & Yezhuvath, U. (2013). Functional connectivity in inhibitory control networks and severity of cannabis use disorder. The American Journal of Drug and Alcohol Abuse, 39(6), 382–391.

12. Fillmore, M. T., & Rush, C. R. (2002). Impaired inhibitory control of behavior in chronic cocaine users. Drug and Alcohol Dependence, 66(3), 265–273.

13. Fischl, B. (2012). Freesurfer. Neuroimage, 62(2), 774–781.

14. Fuster, J. M. (2001). The prefrontal cortex—an update: Time is of the essence. Neuron, 30(2), 319–333.

15. Geisler, D., Walton, E., Naylor, M., Roessner, V., Lim, K. O., Charles Schulz, S., … Ehrlich, S. (2015). Brain structure and function correlates of cognitive subtypes in schizophrenia. Psychiatry Research: Neuroimaging, 234(1), 74–83.

16. Gershon, R. C., Wagster, M. V., Hendrie, H. C., Fox, N. A., Cook, K. F., & Nowinski, C. J. (2013). NIH toolbox for assessment of neurological and behavioral function. Neurology, 80(Issue 11, Supplement 3), S2–S6.

17. Giedd, J. N. (2004). Structural magnetic resonance imaging of the adolescent brain. Annals of the New York Academy of Sciences, 1021(1), 77–85.

18. Glasser, M. F., & Van Essen, D. C. (2011). Mapping human cortical areas In vivo based on myelin content as revealed by T1- and T2-weighted MRI. Journal of Neuroscience, 31(32), 11597–11616.

19. Hampshire, A., & Sharp, D. J. (2015). Contrasting network and modular perspectives on inhibitory control. Trends in Cognitive Sciences, 19(8), 445–452.

20. He, Y., Chen, Z. J., & Evans, A. C. (2007). Small-world anatomical networks in the human brain revealed by cortical thickness from MRI. Cerebral Cortex, 17(10), 2407–2419.

21. Heaton, R. K., Akshoomoff, N., Tulsky, D., Mungas, D., Weintraub, S., Dikmen, S., … Gershon, R. (2014). Reliability and validity of composite scores from the NIH toolbox cognition battery in adults. Journal of the International Neuropsychological Society, 20(06), 588–598.

22. Hoekzema, E., Barba-Müller, E., Pozzobon, C., Picado, M., Lucco, F., García-García, D., … Vilarroya, O. (2016). Pregnancy leads to long-lasting changes in human brain structure. Nature Neuroscience, 20(2), 287–296.

23. Hummer, T. A., Wang, Y., Kronenberger, W. G., Mosier, K. M., Kalnin, A. J., Dunn, D. W., & Mathews, V. P. (2010). Short-term violent video game play by adolescents alters prefrontal activity during cognitive inhibition. Media Psychology, 13(2), 136–154.

24. Ilieva, I. P., Hook, C. J., & Farah, M. J. (2015). Prescription stimulants' effects on healthy inhibitory control, working memory, and episodic memory: A meta-analysis. Journal of Cognitive Neuroscience, 27(6), 1069–1089.

25. Izquierdo, A., & Jentsch, J. D. (2012). Reversal learning as a measure of impulsive and compulsive behavior in addictions. Psychopharmacology, 219(2), 607–620.

26. Koob G. F. & Volkow N. D. (2010). Neurocircuitry of addiction. Neuropsychopharmacology. 35 (1): 217–38.

27. Lerman-Sinkoff, D. B., Sui, J., Rachakonda, S., Kandala, S., Calhoun, V. D., & Barch, D. M. (2017). Multimodal neural correlates of cognitive control in the Human Connectome Project. NeuroImage, 163, 41–54.

28. Li, S., Yuan, X., Pu, F., Li, D., Fan, Y., Wu, L., … Han, Y. (2014). Abnormal changes of multidimensional surface features using multivariate pattern classification in amnestic mild cognitive impairment patients. Journal of Neuroscience, 34(32), 10541–10553.

29. Li, W., Yang, C., Shi, F., Wu, S., Wang, Q., Nie, Y., & Zhang, X. (2017). Construction of individual morphological brain networks with multiple morphometric features. Frontiers in Neuroanatomy, 11–34.

30. Liddle, E. B., Hollis, C., Batty, M. J., Groom, M. J., Totman, J. J., Liotti, M., … Liddle, P. F. (2010). Task-related default mode network modulation and inhibitory control in ADHD: effects of motivation and methylphenidate. Journal of Child Psychology and Psychiatry, 52(7), 761–771.

31. Lim, H. K., Jung, W. S., Ahn, K. J., Won, W. Y., Hahn, C., Lee, S. Y., … Lee, C. U. (2012). Regional cortical thickness and subcortical volume changes are associated with cognitive impairments in the drug-naive patients with late-onset depression. Neuropsychopharmacology, 37(3), 838–849.

32. Luo, X.. (2001). Basic neuroscience. Central South University Press.

33. Maij, D. L., van de Wetering, B. J., & Franken, I. H. (2017). Cognitive control in young adults with cannabis use disorder: An event-related brain potential study. Journal of Psychopharmacology, 31(8), 1015–1026.

34. Metzuyanim-Gorlick, S., & Mashal, N. (2016). The effects of transcranial direct current stimulation over the dorsolateral prefrontal cortex on cognitive inhibition. Experimental Brain Research, 234(6), 1537–1544.

35. Morasch, K. C., & Bell, M. A. (2011). The role of inhibitory control in behavioral and physiological expressions of toddler executive function. Journal of Experimental Child Psychology, 108(3), 593–606.

36. Mostofsky, S. H., Newschaffer, C. J., & Denckla, M. B. (2003). Overflow movements predict impaired response inhibition in children with ADHD. Perceptual and Motor Skills, 97(3_suppl), 1315–1331.

37. Neubert, F.-X., Mars, R. B., Thomas, A. G., Sallet, J., & Rushworth, M. F. S. (2014). Comparison of human ventral frontal cortex areas for cognitive control and language with areas in monkey frontal cortex. Neuron, 81(3), 700–713.

38. Niendam, T. A., Laird, A. R., Ray, K. L., Dean, Y. M., Glahn, D. C., & Carter, C. S. (2012). Meta-analytic evidence for a superordinate cognitive control network subserving diverse executive functions. Cognitive, Affective, & Behavioral Neuroscience, 12(2), 241–268.

39. Noonan, M. P., Chau, B. K. H., Rushworth, M. F. S., & Fellows, L. K. (2017). Contrasting effects of medial and lateral orbitofrontal cortex lesions on credit assignment and decision-making in humans. The Journal of Neuroscience, 37(29), 7023–7035.

40. Norman, A. L., Pulido, C., Squeglia, L. M., Spadoni, A. D., Paulus, M. P., & Tapert, S. F. (2011). Neural activation during inhibition predicts initiation of substance use in adolescence. Drug and Alcohol Dependence, 119(3), 216–223.

41. Öngür, D., Ferry, A. T., & Price, J. L. (2003). Architectonic subdivision of the human orbital and medial prefrontal cortex. The Journal of Comparative Neurology, 460(3), 425–449.

42. Panizzon, M. S., Fennema-Notestine, C., Eyler, L. T., Jernigan, T. L., Prom-Wormley, E., Neale, M., … Kremen, W. S. (2009). Distinct genetic influences on cortical surface area and cortical thickness. Cerebral Cortex, 19(11), 2728–2735.

43. Pienaar, R., Fischl, B., Caviness, V., Makris, N., & Grant, P. E. (2008). A methodology for analyzing curvature in the developing brain from preterm to adult. International Journal of Imaging Systems and Technology, 18(1), 42–68.

44. Pires, L., Leitão, J., Guerrini, C., & Simões, M. R. (2014). Event-related brain potentials in the study of inhibition: Cognitive control, source localization and age-related modulations. Neuropsychology Review, 24(4), 461–490.

45. Power, J. D., Cohen, A. L., Nelson, S. M., Wig, G. S., Barnes, K. A., Church, J. A., … Petersen, S. E. (2011). Functional network organization of the human brain. Neuron, 72(4), 665–678.

46. Qi, X., Xu, F., & Fan, Z. (2017). Analysis of sMRI features of mild cognitive impairment and Alzheimer disease. China Modern Medicine.

47. Rimol, L. M., Nesvåg, R., Hagler, D. J., Bergmann, Ø., Fennema-Notestine, C., Hartberg, C. B., … Dale, A. M. (2012). Cortical volume, surface area, and thickness in schizophrenia and bipolar disorder. Biological Psychiatry, 71(6), 552–560.

48. Rolls, E. T. (2016) Cerebral cortex: principles of operation. Oxford University Press: Oxford.

49. Rolls, E. T. (2017) The orbitofrontal cortex and emotion in health and disease, including depression. Neuropsychologia, S0028-3932(17)30347–0.

50. Rolls, E. T. (2018) The brain, emotion, and depression. Oxford University Press: Oxford.

51. Rolls, E. T. (2019) The orbitofrontal cortex. Oxford University Press.

52. Rosenberg, M. D., Hsu, W.-T., Scheinost, D., Todd Constable, R., & Chun, M. M. (2018). Connectome-based models predict separable components of attention in novel individuals. Journal of Cognitive Neuroscience, 30(2), 160–173.

53. Sabuncu, M. R., Ge, T., Holmes, A. J., Smoller, J. W., Buckner, R. L., & Fischl, B. (2016). Morphometricity as a measure of the neuroanatomical signature of a trait. Proceedings of the National Academy of Sciences, 113(39), E5749–E5756.

54. Schaer, M., Cuadra, M. B., Tamarit, L., Lazeyras, F., Eliez, S., & Thiran, J.-P. (2008). A surface-based approach to quantify local cortical gyrification. IEEE Transactions on Medical Imaging, 27(2), 161–170.

55. Schaer, M., Cuadra, M. B., Schmansky, N., Fischl, B., Thiran, J.-P., & Eliez, S. (2012). How to measure cortical folding from MR Images: A step-by-step tutorial to compute local gyrification index. Journal of Visualized Experiments, (59).

56. Seidlitz, J., Váša, F., Shinn, M., Romero-Garcia, R., Whitaker, K. J., Vértes, P. E., … Bullmore, E. T. (2018). Morphometric similarity networks detect microscale cortical organization and predict inter-individual cognitive variation. Neuron, 97(1), 231–247.e7.

57. Sellitto, M., Ciaramelli, E., & di Pellegrino, G. (2010). Myopic discounting of future rewards after medial orbitofrontal damage in humans. Journal of Neuroscience, 30(49), 16429–16436.

58. Shen, X., Finn, E. S., Scheinost, D., Rosenberg, M. D., Chun, M. M., Papademetris, X., & Constable, R. T. (2017). Using connectome-based predictive modeling to predict individual behavior from brain connectivity. Nature Protocols, 12(3), 506–518.

59. Shimoda, K., Kimura, M., Yokota, M., & Okubo, Y. (2015). Comparison of regional gray matter volume abnormalities in Alzheimer′s disease and late life depression with hippocampal atrophy using VSRAD analysis: A voxel-based morphometry study. Psychiatry Research: Neuroimaging, 232(1), 71–75.

60. Smid, H. G.,Böcker, K. B., van Touw, D. A., Mulder, G., & Brunia, C. H. (1996). A psychophysiological investigation of the selection and the use of partial stimulus information in response choice. Journal of Experimental Psychology: Human Perception and Performance, 22(1), 3–24.

61. Sowell, E. R., Trauner, D. A., Gamst, A., & Jernigan, T. L. (2007). Development of cortical and subcortical brain structures in childhood and adolescence: a structural MRI study. Developmental Medicine & Child Neurology, 44(1), 4–16.

62. Stange, J. P., Bessette, K. L., Jenkins, L. M., Peters, A. T., Feldhaus, C., Crane, N. A., … Langenecker, S. A. (2017). Attenuated intrinsic connectivity within cognitive control network among individuals with remitted depression: Temporal stability and association with negative cognitive styles. Human Brain Mapping, 38(6), 2939–2954.

63. Szatkowska, I., Szymańska, O., Bojarski, P., & Grabowska, A. (2007). Cognitive inhibition in patients with medial orbitofrontal damage. Experimental Brain Research, 181(1), 109–115.

64. Tofallis, C. (2015). A better measure of relative prediction accuracy for model selection and model estimation. Journal of the Operational Research Society, 66(8), 1352–1362.

65. Van Essen, D. C., Smith, S. M., Barch, D. M., Behrens, T. E. J., Yacoub, E., & Ugurbil, K. (2013). The WU-Minn Human Connectome Project: An overview. NeuroImage, 80, 62–79.

66. Vandekar, S. N., Shinohara, R. T., Raznahan, A., Hopson, R. D., Roalf, D. R., Ruparel, K., … Satterthwaite, T. D. (2016). Subject-level measurement of local cortical coupling. NeuroImage, 133, 88–97.

67. Walton, M. E., Behrens, T. E. J., Buckley, M. J., Rudebeck, P. H., & Rushworth, M. F. S. (2010). Separable Learning Systems in the Macaque Brain and the Role of Orbitofrontal Cortex in Contingent Learning. Neuron, 65(6), 927–939.

68. Watson, A. J., & Bell, M. A. (2013). Individual differences in inhibitory control skills at three years of age. Developmental Neuropsychology, 38(1), 1–21.

69. Weintraub, S., Dikmen, S. S., Heaton, R. K., Tulsky, D. S., Zelazo, P. D., Bauer, P. J., … Gershon, R. C. (2013). Cognition assessment using the NIH Toolbox. Neurology, 80(Issue 11, Supplement 3), S54–S64.

70. Whitaker, K., Vértes, P., Romero-Garcia, R., Váša, F., Moutoussis, M., Prabhub, G., … Bullmore, E. (2017). Adolescence is associated with genomically patterned consolidation of the hubs of the human brain connectome. Biological Psychiatry, 81(10), S152–S153.

71. Wong, A. W. K., Chen, C., Baum, M. C., Heaton,R. K., Goodman, B., & Heinemann, A. W. (2019). Cognitive, emotional, and physical functioning as predictors of paid employment in people with stroke, traumatic brain injury, and spinal cord injury. American Journal of Occupational Therapy, 73(2):7302205010p1–7302205010p15.

72. Yokota, S., Takeuchi, H., Hashimoto, T., Hashizume, H., Asano, K., Asano, M., … Kawashima, R. (2015). Individual differences in cognitive performance and brain structure in typically developing children. Developmental Cognitive Neuroscience, 14, 1–7.

73. Yu, K., Wang, X., Li, Q., Zhang, X., Li, X., & Li, S. (2018). Individual morphological brain network construction based on multivariate euclidean distances between brain regions. Frontiers in Human Neuroscience, 12.

74. Zelazo, P. D., Anderson, J. E., Richler, J., Wallner-Allen, K., Beaumont, J. L., & Weintraub, S. (2013). II. NIH Toolbox Cognition Battery (CB): Measuring executive function and attention. Monographs of the Society for Research in Child Development, 78(4), 16–33.

75. Zelazo, P. D., Anderson, J. E., Richler, J., Wallner-Allen, K., Beaumont, J. L., Conway, K. P., … Weintraub, S. (2014). NIH Toolbox Cognition Battery (CB): Validation of executive function measures in adults. Journal of the International Neuropsychological Society, 20(06), 620–629.